

CHEMICAL KINETICS  
AND CATALYSIS

# Catalytic Hydrogenation of Carbon Monoxide over Nanostructured Perovskite-Like Gadolinium and Strontium Ferrites

T. F. Sheshko<sup>a</sup>, Yu. M. Serov<sup>a</sup>, M. V. Dement'eva<sup>a</sup>, A. Shul'ga<sup>a</sup>, I. V. Chislova<sup>b</sup>, and I. A. Zvereva<sup>b</sup>

<sup>a</sup>Peoples' Friendship University, Moscow, 117198 Russia

<sup>b</sup>St. Petersburg State University, St. Petersburg, 199034 Russia

e-mail: sheshko\_tf@pfur.ru

Received July 13, 2015

**Abstract**—The catalytic properties of perovskite-like ferrites ( $A_{n+1}B_nO_{3n+1}$ , where  $n = 1, 2, 3, \dots, \infty$ ;  $A = \text{Gd, Sr}$ ; and  $B = \text{Fe}$ ) synthesized via ceramic and sol-gel technology in the hydrogenation of carbon monoxide are studied. The interrelation between catalytic activity, selectivity to olefins and synthetic methods for complex oxide preparation, the number of perovskite layers, crystallite size, composition, and the valence state of iron is established.

**Keywords:** carbon monoxide, hydrogenation, ferrites.

**DOI:** 10.1134/S0036024416050277

## INTRODUCTION

Commercially important organic compounds, e.g., ethylene and propylene, can be prepared via multiple synthetic pathways using carbon monoxide and hydrogen as the initial substances. Such synthesis is thus of both applied and theoretical interest. The production of gaseous olefins is especially important, since it makes chemical industry less dependent on gasoline supplies. Well-known industrially tested synthetic processes based on carbon oxides (particularly the Fischer–Tropsch process) produce a wide variety of chemical products (with respect to the number of carbon atoms). These products are characterized by different contents of olefin in the individual hydrocarbon fractions. Improving selectivity by regulating their carbon content (the predetermined hydrocarbon chain length) is therefore an important line of research. The development and creation of efficient noble metal-free catalytic systems for the conversion of emissions containing both oxides to olefins at atmospheric pressure is of great relevance.

Complex layered perovskite-like oxides, including ferrites, have a unique set of physical and chemical properties, e.g., mixed ionic–electronic conductivity and high mechanical strength and heat resistance. However, the catalytic properties of these materials remain poorly studied.

The aim of this work was to study the catalytic activity and selectivity of perovskite-like gadolinium and strontium ferrites in the hydrogenation of carbon monoxide at atmospheric pressure, and to determine the effect the method of preparation, structure, and

composition of complex oxides have on their catalytic activity.

## EXPERIMENTAL

Ferrites  $\text{GdFeO}_3$ ,  $\text{SrFeO}_{3-x}$ ,  $\text{GdSrFeO}_4$ , and  $\text{Gd}_2\text{SrFe}_2\text{O}_7$  were synthesized via the solid-phase and sol–gel routes described in [1–3]. The phase composition in the crystal structures of the synthesized samples was studied via X-ray diffraction using an ARL X'TRA diffractometer with  $\text{CuK}\alpha$  radiation. Sample images were obtained using Zeiss EVO<sup>®</sup>40 and Carl Zeiss Supra 40VP scanning electron microscopes at accelerating voltages of 10 and 20 kV, respectively. The average particle size and particle size distribution were determined using a Malvern Zetasizer Nano analyzer with a 4 mW helium–neon laser operating at a wavelength of 633 nm. All measurements were made using closed disposable polystyrene cuvettes at 293 K. The particle size distribution in units of intensity was obtained via correlation function analysis using the Multiple Narrow Modes algorithm in the analyzer software.

The sample surface was analyzed via low temperature nitrogen adsorption at  $T = 77$  K using a Nova 4200E (Quantachrome) device. Adsorption–desorption isotherms were used to determine the specific surface area by BET and to estimate the pore size.

Mössbauer spectra were recorded at room temperature using a Wissel spectrometer ( $^{57}\text{Co}$  in a rhodium matrix with an activity of 10 mCi); isomer shifts were calculated with respect to  $\alpha\text{-Fe}$ . The intensity of the signals was determined within the accuracy of the

**Table 1.** Rates of methane and ethylene formation, selectivity to olefins, and the experimental activation energies and pre-exponential factors for strontium and gadolinium ferrites (c denotes ceramic technology; s–g, sol–gel synthesis)

Ferrite	$n$	$W$ , mmol/(h g <sub>cat</sub> ), 673 K CO : H <sub>2</sub> = 1 : 2		$S$ (C <sub>n</sub> H <sub>2n</sub> ), % 673–708 K	$E_a$ (CH <sub>4</sub> ), kJ/mol		Ln ln $K_0$ (CH <sub>4</sub> )		$E_a$ (C <sub>2</sub> H <sub>4</sub> ), kJ/mol		Ln ln $K_0$ (C <sub>2</sub> H <sub>4</sub> )	
		CH <sub>4</sub>	C <sub>2</sub> H <sub>4</sub>		$T < T^*$	$T > T^*$	$T < T^*$	$T > T^*$	$T < T^*$	$T > T^*$	$T < T^*$	$T > T^*$
SrFeO <sub>3-x</sub>	∞	4.12	0.1	10.2	46		3		48		-1	
GdFeO <sub>3</sub> (c)	∞	4.1	1.26	13.8	96	60	12.5	5.4	90	50	10.5	1.7
GdFeO <sub>3</sub> (s–g)	∞	4.7	4.4	16.3	106	48	15.2	3.6	97	72	12.1	7.4
Gd <sub>2</sub> SrFe <sub>2</sub> O <sub>7</sub>	2	5.2	2.95	36.1	98	40	13.8	2.4	67	54	6.9	1.4
GdSrFeO <sub>4</sub>	1	1.1	0.44	35.7	96	86	9.5	12.7	86	80	6.5	9.1
Fe <sub>2</sub> O <sub>3</sub>	–	34.6	2.48	8.2	35		3.1		31		-0.4	

$T^* = 548\text{--}598$  K.

resonance absorption coefficient in order to assess the contribution from paramagnetic particles.

Catalytic activity was determined in a reactor with gas mixtures in component ratios [CO : H<sub>2</sub>] = 1 : 1, 1 : 2, and 1 : 4. The experiments were performed in a flow catalytic setup at atmospheric pressure and volumetric rates of 1.5–3.0 L/h, in the temperature range of 423–723 K. To avoid sintering, ferrite powders were mixed with a fine quartz powder ( $d_{av} = 1\text{--}10$  μm) in a ratio of 1 : 1; 0.2–0.3 g of each catalyst was placed into a quartz reactor (diameter, 1 cm) with a quartz filter, preventing particle carryover. The products were ana-

lyzed chromatographically using a Crystall 5000 device equipped with a stainless steel column filled with Porapak Q at 393 K. Thermal conductivity and flame ionization detectors connected in sequence were also used. The rate of reaction product formation ( $W$ , mol/(h g<sub>cat</sub>)) or the specific catalytic activity (SCA) was measured after a steady state was achieved; i.e., the areas of the chromatographic peaks remained constant.

For catalytic properties of the complex oxides A<sub>n+1</sub>B<sub>n</sub>O<sub>3n+1</sub> ( $n = 1, 2, 3, \dots, \infty$ ; A = Gd, Sr; B = Fe) to be evaluated, the iron (III) oxide powder (chemically pure grade, iron oxide content 99.9%) was tested as a catalyst for comparison.

## RESULTS AND DISCUSSION

The studied ferrites are classified as Ruddlesden–Popper phases [4]. The structure of these compounds is block-like and consists of interpenetrating perovskite (P) ABO<sub>3</sub> and rock salt (RS) AO fragments with a number of alternating layers ... (P)(P)(RS)(P)(P)(RS)..... (Fig. 1).

Using X-ray analysis, one phase with a perovskite-like layered structure was found in GdFeO<sub>3</sub>, GdSrFeO<sub>4</sub>, and Gd<sub>2</sub>SrFe<sub>2</sub>O<sub>7</sub> prepared via both the solid-phase and the sol–gel techniques. A comparison of the diffraction reflections and the determination of CSR showed the particles of the polycrystalline samples prepared using ceramic technology to be bigger than those of the same compound obtained with the sol–gel method.

According to photon correlation spectroscopy and scanning electron microscopy data (Fig. 2), the particles were anisotropic, and the average diameter and length of the crystallites synthesized according to the ceramic technique were 2–10 and 10 μm, respectively. For the sol–gel products, these parameters were 30–60 and 200 nm, respectively. It should be noted that the particle morphology also differed: the shape of the

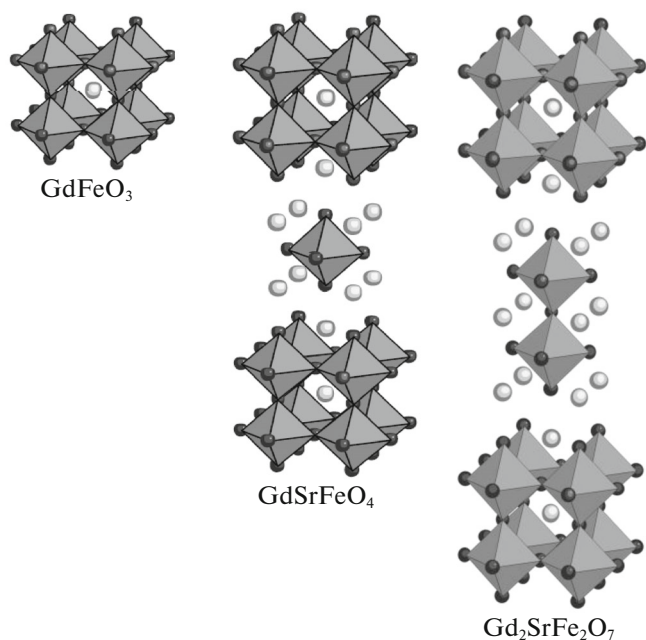


**Fig. 1.** Structures of distorted perovskite ferrite GdFeO<sub>3</sub>, layered oxide GdSrFeO<sub>4</sub>, and layered oxide Gd<sub>2</sub>SrFe<sub>2</sub>O<sub>7</sub> (o, denotes Sr<sup>2+</sup>, Gd<sup>3+</sup>, Fe<sup>3+</sup> lies inside the octahedron).

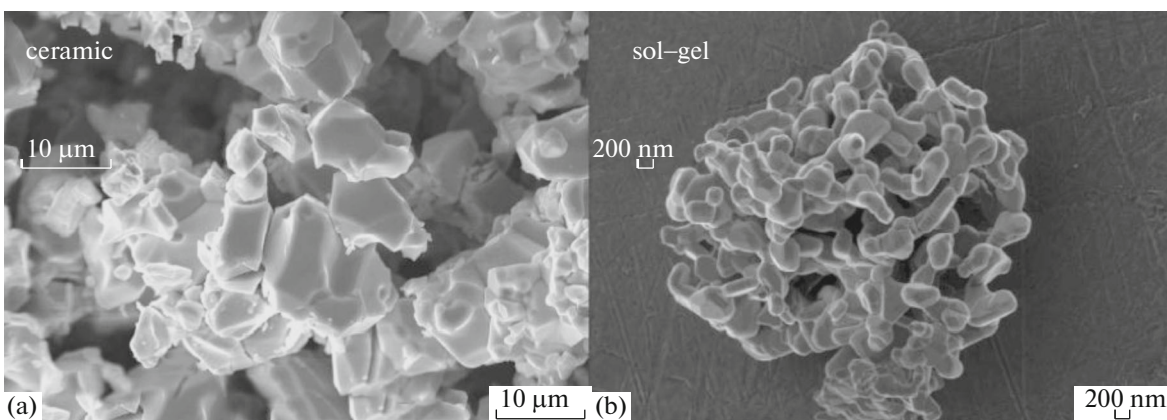


**Fig. 2.** SEM images of complex layered oxide  $Gd_2SrFe_2O_7$ , prepared via ceramic technology and the sol-gel method.

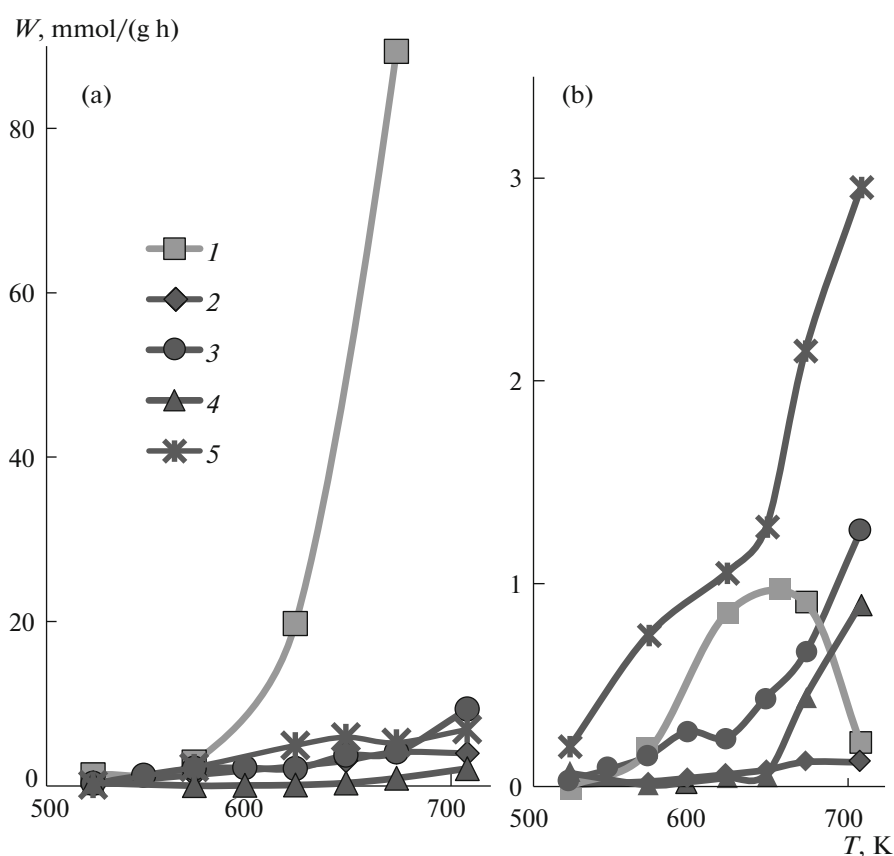


**Fig. 3.** Temperature dependence of the rate of (a) methane and (b) ethylene formation at the ratio  $CO : H_2 = 1 : 2$  on (1)  $Fe_2O_3$ , (2)  $SrFeO_{3-x}$ , (3)  $GdFeO_3$ , (4)  $GdSrFeO_4$ , and (5)  $Gd_2SrFe_2O_7$ .

particles prepared via the sol-gel method was uniform, as was the particle size distribution. In addition, the samples all had porous surfaces.

According to the Mössbauer spectroscopy data, the iron atoms in the complex ferrites prepared using ceramic technology were in a magnetically ordered state,  $Fe^{3+}$ . Mössbauer spectra of the solid solutions synthesized via sol-gel technology showed the iron

atoms in the  $GdFeO_3$  samples to be in state  $Fe^{3+}$  in two fields with different symmetry. In the case of complex oxides  $GdSrFeO_4$  and  $Gd_2SrFe_2O_7$ , there were not only  $Fe^{3+}$  atoms in three fields with different symmetry but also  $Fe^{4+}$  with oxygen vacancies. The  $Fe^{4+}$  content in  $GdSrFeO_4$  samples was 17%; in  $Gd_2SrFe_2O_7$ , it was 13%. Two iron forms were found in  $SrFeO_{3-x}$ :  $Fe^{3+}$  in two symmetry fields plus  $Fe^{4+}$  (27%). The

**Table 2.** Content of CO and CO<sub>2</sub> in the gas phase at 673 K, and CO conversion in the range 573–673 K (the reaction was conducted at the ratio CO : H<sub>2</sub> = 1 : 2)

Catalyst		Fe <sub>2</sub> O <sub>3</sub>	SrFeO <sub>3-x</sub>	GdFeO <sub>3</sub>	GdSrFeO <sub>4</sub>	Gd <sub>2</sub> SrFe <sub>2</sub> O <sub>7</sub>
N(CO) <sub>673</sub> , mmol/(g h)		54	20	80	132	88
N(CO <sub>2</sub> ) <sub>673</sub> , mmol/(g h)		27	15	17	43	25
α (CO), %	573 K	45	76	40	57	57
	623 K	59	76	45	57	57
	673 K	81	76	48	56	57

reduced Fe<sup>3+</sup> symmetry is explained by the presence of oxygen vacancies. Additional state of the iron atoms can be stabilized on the surfaces of the crystallites, where the oxygen environment is most distorted and the Fe<sup>3+</sup> atoms lie in the region of lower symmetry.

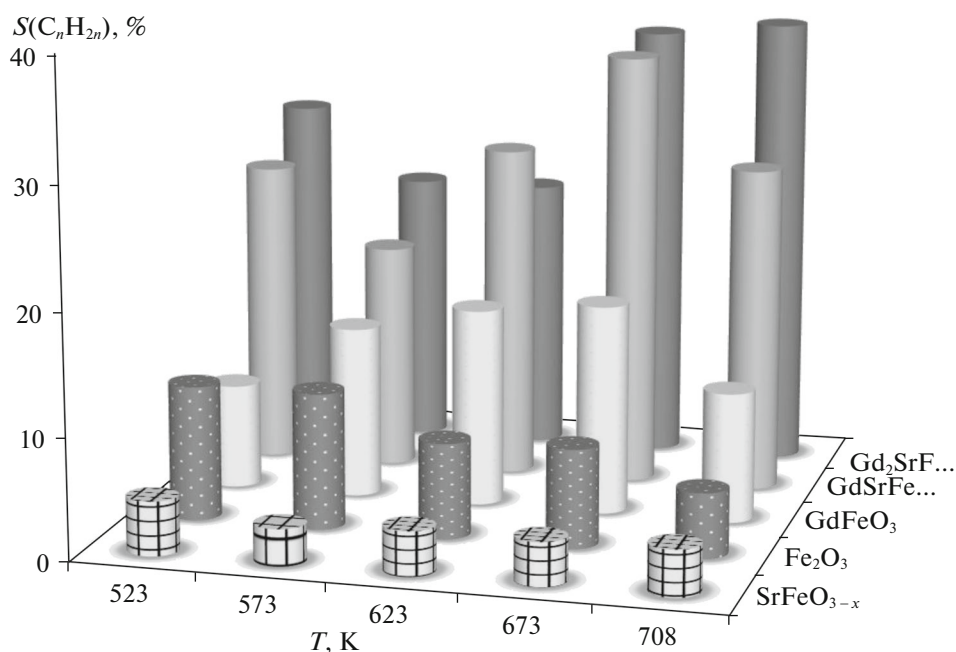
The hydrogenation of carbon monoxide at initial product ratios CO : H<sub>2</sub> = 1 : 1, 1 : 2, and 1 : 4 on Fe<sub>2</sub>O<sub>3</sub>, SrFeO<sub>3-x</sub>, GdFeO<sub>3</sub>, GdSrFeO<sub>4</sub>, Gd<sub>2</sub>SrFe<sub>2</sub>O<sub>7</sub> resulted in the formation of C<sub>1</sub>–C<sub>5</sub> hydrocarbons. The reaction began at 523 K, and its rate increased with temperature. When Fe<sub>2</sub>O<sub>3</sub> was used as a catalyst, the main reaction product was methane, with the content of other hydrocarbons being much less. The use of complex oxides A<sub>n+1</sub>Fe<sub>n</sub>O<sub>3n+1</sub> led to a sharp drop in methane formation, its content being comparable to that of ethylene (Fig. 3). The same qualitative composition of the reaction products was observed when the H<sub>2</sub> content in the reaction mixture was reduced from the ratio CO : H<sub>2</sub> = 1 : 4 to CO : H<sub>2</sub> = 1 : 1. However, the product ratio was different, since there was a sig-

nificant increase in the olefin content and only a slight change in the methane content. For all of the studied perovskite-like samples, the maximum rate of ethylene and propylene formation was observed at the ratio CO : H<sub>2</sub> = 1 : 2.

A comparison of the rates of product formation on the samples prepared via the sol–gel method (Table 1) showed that the specific catalytic activity with respect to methane grew in the order GdSrFeO (*n* = 1) < SrFeO<sub>3-x</sub> (*n* = ∞) ≤ GdFeO<sub>3</sub> (*n* = ∞) < Gd<sub>2</sub>SrFe<sub>2</sub>O<sub>7</sub> (*n* = 2).

The use of the complex oxides as catalysts resulted in considerably greater selectivity toward ethylene and propylene, relative to Fe<sub>2</sub>O<sub>3</sub> (Fig. 4). At 673 K, the highest *S*(C<sub>*n*</sub>H<sub>2*n*</sub>) values of 17, 36, and 38% were obtained at CO : H<sub>2</sub> = 1 : 2 ratio on GdFeO<sub>3</sub>, GdSrFeO<sub>4</sub>, and Gd<sub>2</sub>SrFe<sub>2</sub>O<sub>7</sub>, respectively.

Analysis of the catalyst structure and composition, and of the selectivity toward ethylene and propylene, showed that the content of light olefins grew after SrO

**Fig. 4.** Temperature dependence of the all selectivities toward olefins at the ratio CO : H<sub>2</sub> = 1 : 2.

was introduced into  $\text{GdFeO}_3$ . Selectivity toward olefins on perovskite-like ferrites reached 40% and increased in the order  $\text{SrFeO}_{3-x}$  ( $n = \infty$ )  $<$   $\text{Fe}_2\text{O}_3$   $<$   $\text{GdFeO}_3$  ( $n = \infty$ )  $<$   $\text{GdSrFeO}_4$  ( $n = 1$ )  $<$   $\text{Gd}_2\text{SrFe}_2\text{O}_7$  ( $n = 2$ ).

In contrast to iron oxide, two linear regions were observed on the Arrhenius dependences of the rates of product formation when using gadolinium ferrites as catalysts. The presence of the two linear regions with different activation energies  $E_a$  can be explained by the change in active centers  $\text{Me}^{n+}$  as a result of the altered temperature of the state or by the change of the reaction mechanism. Temperature  $T^*$  at the bend was calculated using the formula  $T^* = \frac{a_1 - a_2}{b_2 - b_1}$  as the solution

to a system of two equations:  $y = a + bx$ , where  $a$  is the logarithm of the pre-exponential factor,  $b = E_a/R$ . The  $E_a$  values for methane and ethylene formation changed upon the transition at  $T^* = 523\text{--}548$  K (Table 1). This could have been due to a change in the mode of carbon monoxide adsorption. At temperatures lower than  $T^*$ , the mode of CO adsorption on the active catalytic centers is linear [5]; when  $T > T^*$ , it is a bridge (probably carboxylate) mode on  $\text{Me}^{n+}\text{--Me}^0$  centers with stronger bonds (heat of adsorption,  $Q_{\text{ads}}$ ). The experimental value of the reaction activation energy thus fell upon the transition at  $T^*$  according to the well-known Polani–Semenov correlation  $E_a = E_{0a} - \alpha Q_A$ , where  $Q_A$  is the heat of chemical transformation,  $E_{0a}$  is the true activation energy of the reaction, and  $\alpha Q_A$  is the contribution from the heat effect.

In addition, oxides  $\text{SrFeO}_{3-x}$ ,  $\text{GdFeO}_3$ ,  $\text{GdSrFeO}_4$ , and  $\text{Gd}_2\text{SrFe}_2\text{O}_7$  are supposed to have several types of active sites, some of which work at temperatures lower than 548 K while others work at higher temperatures. As was mentioned above, the iron atoms in complex oxide  $\text{GdFeO}_3$  are in the  $\text{Fe}^{3+}$  state in two fields of different symmetry, while  $\text{Fe}^{4+}$  with oxygen vacancies is found in layered oxides  $\text{SrFeO}_{3-x}$ ,  $\text{GdSrFeO}_4$ , and  $\text{Gd}_2\text{SrFe}_2\text{O}_7$ , in addition to  $\text{Fe}^{3+}$  in fields of different symmetries. The heterovalent coordinatively unsaturated state of iron could be another reason for the emergence of different active catalytic sites.

The ratio of paraffins and olefins in the reaction products was mainly determined by the amount of atomic hydrogen able to migrate from one active surface site to another [6, 7]. As was shown in [6, 8, 9], two forms of chemisorbed hydrogen can exist on a metal surface:  $\text{H}_I$  (weakly bound) and  $\text{H}_{II}$  (strongly adsorbed). Hydrocarbons form via a stage of active carbon formation, but the selectivity of the process toward olefins is determined by the  $\text{H}_I : \text{H}_{II}$  ratio on the catalyst's surface. The non-isovalent substitution of  $\text{Gd}^{3+}$  for  $\text{Sr}^{2+}$  is likely to distort the perovskite structure, reduce the symmetry of iron atoms, and lead to the emergence of oxygen vacancies. Most of the labile

atomic hydrogen goes for the partial reduction of  $\text{Fe}^{4+}$  to  $\text{Fe}^{3+}$ ; i.e., the heterovalent state of iron atoms favors the formation of an unsaturated compound. At the same time, a sample's  $\text{Fe}^{4+}$  content is greatest in  $\text{SrFeO}_{3-x}$ , and the selectivity toward olefins is minimal. This can be explained by the lack of free atomic hydrogen and a reduction in the number of  $\text{Fe}^{3+}$  sites active toward olefins.

Perovskite-like gadolinium ferrite prepared using ceramic technology was tested to determine the effect the method of a catalyst's preparation has on its activity. The composition of the reaction products was the same (C1–C5 hydrocarbons), but the component ratio was different. A substantial drop in the rate of ethylene formation was observed, the rates of methane formation being close at all CO and  $\text{H}_2$  ratios in the reaction mixture (Table 1, Fig. 3).

The differences between the catalytic properties of the samples obtained by various methods could be due to several reasons. First, the samples obtained using ceramic technology were sub-microcrystalline, while ferrites synthesized with the sol–gel process were nanocrystalline with a porous structure that facilitated the transfer of atomic hydrogen and the  $\text{CH}_x$ -particles formed in the reaction from one site to another. Second, as was noted above, the heterovalent state of the iron atoms suitable for the formation of olefins was observed only for sol–gel products.

The content of reactant in the gas phase near the catalyst surfaces was analyzed. It was shown that there was intense adsorption of CO at room temperature, and the shape of the curve was identical for all of the studied samples. After adsorption equilibrium was achieved, the composition of the gas phase ( $\text{CO} + \text{H}_2$ ) was stable up to 573 K, and the subsequent rise in temperature and transition to the catalytic range was accompanied by the formation of  $\text{CO}_2$  (Table 2). CO conversion on all gadolinium-containing ferrites was thus 55–75% and varied only slightly with temperature. It was higher on  $\text{Fe}_2\text{O}_3$  when the reaction was conducted in both a deficit and a surfeit of hydrogen.

The temperature dependences of the carbon oxide content in the reaction mixture when conducting the process in stoichiometric amounts and a deficit of hydrogen on the catalysts were found to be similar, with CO conversion being nearly the same. We may therefore assume that only carbon particles resulting from the dissociative adsorption of carbon monoxide at noncatalytic temperatures were involved in the formation of reaction products.

$\text{CO}_2$  can form as a result of the interaction between adsorbed molecules of CO (ads.) and either perovskite surface oxygen (O (S)) or oxygen released upon the dissociative adsorption of CO:



It should be noted that a drop in  $\text{Fe}_2\text{O}_3$  catalytic activity was observed in repeated experiments, while all results were reproducible for perovskite-like ferrites. When using iron(III) oxide, a considerable amount of the carbon formed during the dissociative adsorption of CO is probably inactive. The catalyst is therefore deactivated due to its carbonization.

### CONCLUSIONS

We established the relationship between catalytic activity and selectivity to olefins and the methods of synthesizing complex oxides, the number of perovskite layers, the size of crystallites, the composition and valence state of iron by studying catalytic properties in the hydrogenation of carbon monoxide perovskite-like ferrites ( $\text{A}_{n+1}\text{B}_n\text{O}_{3n+1}$ , where  $n = 1, 2, 3, \dots, \infty$ ; A = Gd, Sr; B = Fe) synthesized via ceramic and sol-gel technology. The catalytic activity (rate of product formation) was shown to depend on the number of alternating perovskite layers. Ferrites synthesized by the sol-gel method had higher catalytic performance, due to their nanocrystalline state with a porous structure, and to the heterovalent state of the iron atoms ( $\text{Fe}^{3+}$ ,  $\text{Fe}^{4+}$ ), which favored CO activation leading to the formation of  $\text{C}^*$  and  $\text{CH}_x$  radicals.

### ACKNOWLEDGMENTS

This work was supported by the Russian Foundation for Basic Research, project no. 14-03-00940 A.

### REFERENCES

1. I. V. Chislova, A. A. Matveeva, A. V. Volkova, and I. A. Zvereva, *Glass Phys. Chem.* **37**, 653 (2011).
2. I. A. Zvereva, I. V. Otrepina, V. G. Semenov, E. A. Tugova, V. F. Popova, and V. V. Gusarov, *Russ. J. Gen. Chem.* **77**, 972 (2007).
3. I. Chislova, V. Panchuk, et al., *Solid State Phenom.* **194**, 116 (2013).
4. S. N. Ruddlesden and P. Popper, *Acta Crystallogr.* **10**, 538 (1957).
5. N. M. Popova, L. V. Babenkova, and G. A. Savel'eva, *Adsorption and Interaction of Simple Gases with VIII Group Metals* (Nauka, Alma-Ata, 1979) [in Russian].
6. T. F. Sheshko and Yu. M. Serov, *Russ. J. Phys. Chem. A* **86**, 283 (2012).
7. L.-M. Tau, H. A. Dabbagh, B. Chawla, and B. H. Davis, *Catal. Lett.* **7**, 141 (1990).
8. Yu. M. Cerov, Extended Abstract of Doctoral (Chem.) Dissertation (People's Friendship Univ. Russia, Moscow, 1999).
9. M. V. Dementyeva, T. F. Sheshko, and Yu. M. Serov, *Theor. Exp. Chem.* **49**, 46 (2013).

*Translated by D. Yakusheva*